Bull. Chem. Soc. Jpn., 72, 1705—1715 (1999)

High Magnetic Field Effects on the Lifetimes of Radical Pairs Generated by the Photoreduction of Anthraquinone and *n*-Alkyl Anthraquinone-2-carboxylates in Micellar Solutions

Yoshihisa Fujiwara,* Kohji Yoda, Taro Tomonari, Takeshi Aoki, Yukimi Akimoto, and Yoshifumi Tanimoto*

Department of Chemistry, Faculty of Science, Hiroshima University, Kagami-yama, Higashi-Hiroshima 739-8526

(Received December 28, 1998)

The magnetic field effects on the lifetimes of radical pairs (RPs) comprising anthrasemiquinone (AQH·) and alkyl radicals generated in Brij35, HDTCl, and SDS micellar solutions of anthraquinone (AQ) and *n*-alkyl anthraquinone-2-carboxylates (AQ-*n*) were studied by laser flash photolysis in high magnetic fields up to 13 T. The RP lifetimes of AQ and AQ-*n* in the three surfactants increased along with increasing the magnetic field from 0 to about 2 T. The RP lifetimes of AQ in Brij35 and HDTCl drastically decreased in a magnetic field from 3 to 13 T, whereas the RP lifetimes of AQ in SDS were almost constant in the same range of the magnetic field. The increase in the three surfactants was explained by spin-lattice relaxation (SLR) modulated by anisotropic hyperfine and electron dipole–dipole interactions. The drastic decrease in Brij35 and HDTCl was interpreted by SLR modulated by an anisotropic Zeeman interaction. The parameters of the anisotropic *g*-value and the rotational correlation time for an anisotropic Zeeman interaction were obtained. The constant RP lifetimes in SDS at a high magnetic field were interpreted referring to an escape process of AQH· from the micelle core.

Magnetic field effects (MFEs) on photo-induced chemical reactions have been extensively studied over the past two decades.[1—8] In very recent investigations,[9—13] the MFEs in high magnetic fields beyond 2 T using a pulsed magnet and a superconducting magnet have been given some attention, where most of the MFEs have been interpreted by a spin-lattice relaxation (SLR) mechanism. In the SLR mechanism, the MFEs are explained by changes in the SLR transition rates among singlet and triplet states ($T_{\pm1} \longleftrightarrow T_0$ and $T_{\pm1} \longleftrightarrow S$) modulated by the magnetic-field-dependent interactions present in radical pairs (RPs) and biradicals (BRs). Such magnetic interactions as *anisotropic* hyperfine (δhf) and *anisotropic* Zeeman (δg) interactions of the component radicals and electron dipole–dipole (dd) interaction of RPs and BRs must be taken into consideration. Among them, Mukai et al. first showed that a reversal appeared in the magnetic field dependence (MFD) of the BR lifetimes of anthrasemiquinone–CO_2–$(CH_2)_{12}$–OCO–xanthenyl, and pointed out the necessity of introducing both interactions (δhf and δg) with different rotational correlation times.[9b]

To verify the effect of the δhf interaction, it has been experimentally proved that using magnetic isotopes, such as ^{13}C and ^{2}H with nuclear spin, is very helpful. In BRs produced from isotope-substituted benzophenone–CO_2–$(CH_2)_{12}$–O–diphenylmethane and benzophenone–CO_2–$(CH_2)_{12}$–O–phenyl ethanol, Nakagaki et al. showed the importance of the δhf interaction on the BR lifetimes in high magnetic fields (0.1—4 T), and no influence of isotope substitution on lifetimes above 5 T.[10] Using isotope substitution, Fujiwara et al. recently evaluated local magnetic fields, showing the strength of the δhf interactions of BRs (BPH·–O–$(CH_2)_n$–O–BPH·) comprising two equivalent benzophenone (BP) ketyl radicals (BPH·s).[9h] As for the dd interaction, Fujiwara et al. showed that the dd interaction plays an important role in SLR of ^{2}H-substituted BRs of BPH·–O–$(CH_2)_{12}$–O–BPH·, because the importance of δhf interaction is reduced.

However, a systematic, quantitative study of the δg interaction is still being left as a continuing open question. The δg interaction is derived from each radical composing RP, and therefore the δg interaction in RP consists of all of the δg interactions. In a previous paper, where MFDs of RPs generated from BP in micellar solutions were reported,[9g] only a qualitative interpretation of the δg interaction of RPs was mentioned, since only the experimental MFD data of BP were insufficient for interpreting the δg interactions of the component BPH· and alkyl (R·) radicals separately. However, in a comparison with the MFD data of BP, this study on AQ derivatives in micellar solutions could afford quantitative information individually on the δg interactions of anthrasemiquinone (AQH·) and R· radicals, using the strong solute (AQ and BP) and micellar dependence of the MFDs of the RP lifetimes. Changing a solute from BP to AQ in addtion to micellar solvents enhanced the variation in the MFDs useful for a quantitative analysis of δg interaction. The advantage in RPs, not BRs, is that it is facile to vary chromophores related to the photoreaction. Whereas Nakagaki et al. demonstrated that the use of magnetic isotopes, such as ^{13}C and ^{2}H with

nuclear spin, made it possible to investigate the δhf interaction quantitatively,[9h,10] we show in this paper that the strong solute and micellar dependence of MFDs of the RP lifetimes is very effective for evaluating the δg interaction of each component radical in the case of RPs in micellar solutions. Furthermore, a quantitative study on the δg interaction will become helpful for making a clearer distinction between the δg interaction in the SLR mechanism and the Δg mechanism that gives rise to the same effect of decrease on the RP and BR lifetimes in high magnetic fields.

Experimental

Materials. Anthraquinone (AQ) (Nacalai) was purified by recrystallization. The synthesis of *n*-Alkyl Anthraquinone-2-carboxylates (AQ–CO_2–$(CH_2)_{n-1}$–CH_3, n = 2, 3, 4, 6, and 8) (AQ-*n*) (Chart 1) was described in a previous study.[14a] Highly-purified polyoxyethylene (23) lauryl alcohol ether (Brij35), hexadecyltrimetylammonium chloride (HDTCl), sodium dodecyl sulfate (SDS) were used as received from Nacalai. The concentrations of the AQ derivatives, Brij35, HDTCl, and SDS were 0.0013, 0.1, 0.4, and 0.4 mol dm^{-3}, respectively. All aqueous micellar solutions were degassed by several freeze-pump-thaw cycles to remove oxygen.

Apparatus. For determining the RP lifetimes at room temperature, transient absorption signals were measured by a pulse magnet-laser flash photolysis apparatus.[9a,9e] The pump and probe light sources were the third harmonics (355 nm, fwhm 4—6 ns) of a Nd : YAG laser (Spectra-Physics, GCR-11-1) and a Xe arc lamp (Ushio, 150 W), respectively.

Results

Transient Absorption and Reaction Scheme. The transient absorption spectra obtained in the laser photolysis of AQ in a Brij35 micellar solution in the absence of an external magnetic field showed absorption bands at 400 and 700 nm for a 0.16 μs delay and at 380 nm for an 8 μs delay, respectively (Fig. 1). From the literature,[14] the bands at 400 and 700 nm were assigned to the excited triplet state (^{3}AQ*) of AQ and AQH•, whereas the band at 380 nm was ascribed to recombination products in the micelle. Other AQ derivatives (AQ-*n*) showed similar spectra. The reaction scheme in the photoreduction of AQ in a micellar solution is as follows:

$$\mathrm{AQ} \xrightarrow{h\nu\ 355\ \mathrm{nm}} {}^1\mathrm{AQ}^* \quad (1)$$

$${}^1\mathrm{AQ}^* \xrightarrow{\mathrm{ISC}} {}^3\mathrm{AQ}^* \quad (2)$$

$${}^3\mathrm{AQ}^* + \mathrm{RH} \xrightarrow{\text{Hydrogen abstraction}} {}^3[\mathrm{AQH}\cdot + \mathrm{R}\cdot] \quad (3)$$

$${}^3[\mathrm{AQH}\cdot + \mathrm{R}\cdot] \xrightarrow{\text{ISC, SLR}} {}^1[\mathrm{AQH}\cdot + \mathrm{R}\cdot] \quad (4)$$

$${}^3[\mathrm{AQH}\cdot + \mathrm{R}\cdot] \longrightarrow \mathrm{AQH}\cdot + \mathrm{R}\cdot\ (\text{escape radicals}) \quad (5)$$

$${}^3[\mathrm{AQH}\cdot + \mathrm{R}\cdot] \xrightarrow{\text{SO-induced ISC}} \text{Products} \quad (6)$$

$${}^1[\mathrm{AQH}\cdot + \mathrm{R}\cdot] \longrightarrow \mathrm{AQH\text{–}R}\ (\text{recombination products}) \quad (7)$$

^{3}AQ* formed via the excited singlet state (^{1}AQ*) of AQ causes intermolecular hydrogen abstraction to yield the triplet RP ^{3}[AQH• + R•] (^{3}RP) (Eq. 3). ^{3}RP partly undergoes intersystem crossing (ISC) and SLR to the singlet RP ^{1}[AQH• + R•] (^{1}RP) (Eq. 4). Equation 4 consists of ($T_{\pm1}$, T_0)⟷S pathways in the absence of an external magnetic field and $T_{\pm1}$⟷T_0⟷S and $T_{\pm1}$⟷S pathways in the presence of the magnetic field, as shown in Scheme 1. The magnetic field affects the process described by Eq. 4 to change the RP lifetime. ^{3}RP partly generates escape radicals (Eq. 5) and partly disappears to the ground state products via spin-orbit (SO)-induced direct ISC (Eq. 6), which is assumed to be magnetic-field-independent.[15] ^{1}RP produces recombination products as a micellar cage product (Eq. 7). An intramolecular hydrogen abstraction reaction in AQ-*n* was ignored, based on an experimental result that the lifetime (30.4 μs) of ^{3}AQ*-8 in Freon® 113 was extremely long.[14a] Since Freon® 113, which has no hydrogen, is inert toward a hydrogen abstraction reaction, the long lifetime (30.4 μs) means an inefficient intramolecular hydrogen abstraction reaction from its octyl chain. Therefore, the counter radical obtained in this study was considered to be R•, which was generated from the sur-

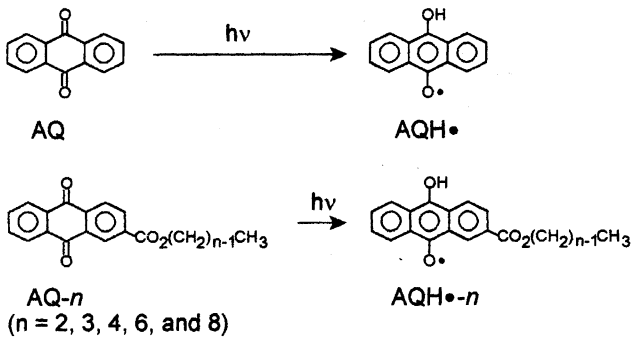

Chart 1.

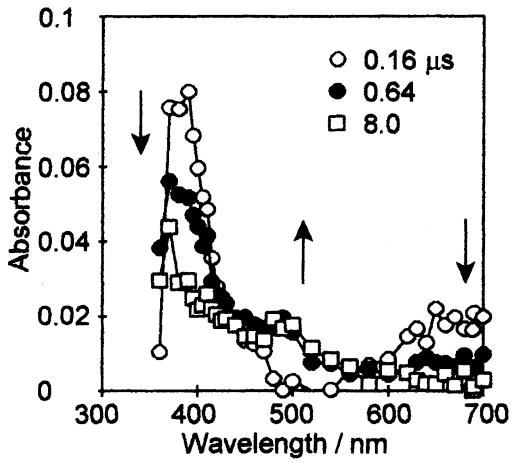

Fig. 1. Time-resolved transient absorption spectra obtained upon photoexcitation of AQ in Brij35 at 0 T.

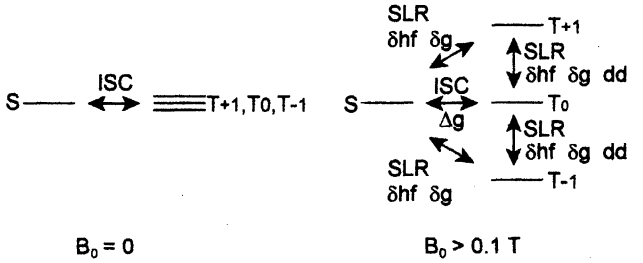

Scheme 1.

factant.

Magnetic Field Effects on RP Lifetimes. Figure 2 shows the transient absorption decay profiles of AQ in Brij35 measured at 400 nm in both the absence and presence of external magnetic fields up to 13 T. These profiles are dependent on the external magnetic field in their decay rates and intensities. At 0 T, the profile at 400 nm consists of three components of two exponential decays (τ_T and τ_{RP} in Eq. 8), in which the pre-exponential factor for the faster decay (τ_T) is very small, and the very long-lived component (A(3) in Eq. 8), which dose not evolve in the time range of the observation (< 35 μs). Figure 2 also depicts the profile at 700 nm at 0 T. Since the profile at 700 nm comprises a large extent of the faster decay, whose lifetime was the same as τ_T at 400 nm, the profile was used for estimating the faster decay time. From the above-mentioned spectral assignments and the fact that the faster decay (τ_T = 154 ns in Brij35, 126 ns in HDTCl, and 335 ns in SDS) was independent of the magnetic field, the faster decay observed at both 400 and 700 nm was referred to ^{3}AQ*. On the other hand, the RP lifetimes (τ_{RP}) in magnetic fields were obtained from the decay profiles at 400 nm, since the absorption at 400 nm was attributed to both ^{3}AQ* and AQH·, as described above. The slower exponential decay (τ_{RP}) and long-lived component (A(3)) at 400 nm were dependent on the magnetic field, and were assigned to the RP and a combination of the escaped AQH· and recombination products, respectively. Hence, the decay profiles at 400 nm were analyzed by the following equation:

$$A(t) = A(1)\ \exp(-t/\tau_T) + A(2)\ \exp(-t/\tau_{RP}) + A(3), \quad (8)$$

where $A(t)$ is the absorbance at time t, τ_T and τ_{RP} are the lifetimes of ^{3}AQ* and RP, and $A(1)$ and $A(2)$ are their pre-exponential factors. Parameter $A(3)$ is the absorbance due to the combination of the escaped AQH· and the recombination products, since the escaped AQH· did not practically decay within the time range of the observation (< 35 μs). The value of τ_T obtained from the decay profile at 700 nm was fixed throughout the analysis of the decay profiles at 400 nm. The signs of the pre-exponential factor $A(1)$ for τ_T were obtained to be negative throughout the analysis of the decay profiles in the presence of a magnetic field, which allows us to understand that the magnetic field dependence in the absorbance at 0 μs of the decay profiles in Fig. 2 results from the major contribution of RP generated at the expense of ^{3}AQ*. The decay profiles of AQH··n, which had similar transient absorption spectra, were analyzed in the same manner. The obtained RP lifetimes of AQ and AQ-n are listed in Table 1, and their MFDs are illustrated in Figs. 3 and 4.

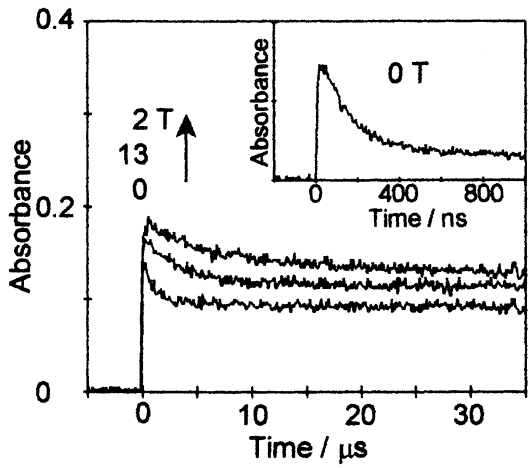

Fig. 2. Decay profiles of transient absorption obtained upon photoexcitation of AQ in Brij35 at magnetic fields of 0, 2, and 13 T monitored at 400 nm. Inset is the decay profile at 0 T monitored at 700 nm.

Brij35. The RP lifetimes in Brij35 at 0 T were 1.6 μs (AQH·), 1.4 μs (AQH··2), 1.5 μs (AQH··3), 1.4 μs (AQH··4), 1.3 μs (AQH··6), and 1.5 μs (AQH··8), respectively, in which no significant difference was observed within the experimental accuracy. The long RP lifetimes at 0 T, compared with that (ca. 200 ns) in a BR consisting of AQH· and xan-

Table 1. RP Lifetimes (μs) Generated from AQ and AQ-n in Micelles at Magnetic Fields[a)]

Quinone	Surfactant	Magnetic field/T							
		0	0.5	1.3	2	3.1	5.7	10	13
AQ	Brij35	1.6	4.6	6.3	6	5.9	5.2	4.3	3.8
AQ	HDTCl	1.5	4.6	9.8	12	9.7	9	8	5.9
AQ	SDS	—[b)]	2.7	3.5	4	3.3	3.9	4	3.9
AQ-2	Brij35	1.4	5	5.6	5.3	5	4.4	3.8	3.6
AQ-3	Brij35	1.5	5.7	5.8	6.6	6	4.8	3.9	4
AQ-4	Brij35	1.4	6.2	6.8	6.9	6.2	5.2	3.7	3.9
AQ-6	Brij35	1.3	6.6	7.2	6.6	6.6	5.3	4.5	4
AQ-8	Brij35	1.5	6.1	7.1	6.9	6.3	5.7	4.3	4.2

a) Experimental error was about 10%. b) The value was not obtained because of the low quantum yield of hydrogen abstraction, as indicated by the long ^{3}AQ* lifetime (335 ns).

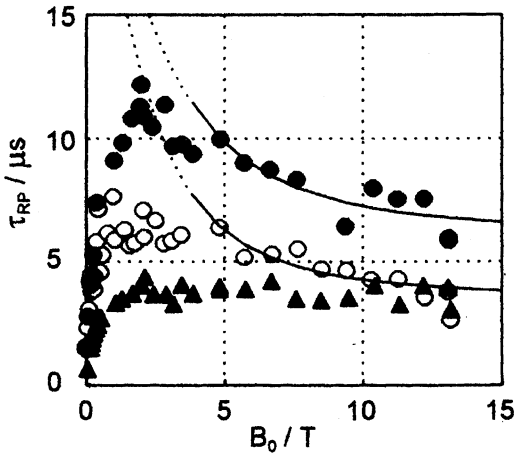

Fig. 3. Observed MFD plots of RP lifetimes of [AQH·+R·] generated in Brij35 (○), HDTCl (●), and SDS (▲). Solid lines in Brij35 and HDTCl were calculated using Eq. 11 with $(g:g)_{(AQH\cdot)} = 4.7\times10^{-6}$, $\tau_{c(AQH\cdot)} = 1.0$ ps, $(g:g)_{(R\cdot)} = 5.3\times10^{-6}$, $\tau_{c(R\cdot)} = 1.1$ ps, and $k_T = 5\times10^4$ s^{-1} and using Eq. 13 with $(g:g)_{(AQH\cdot)} = 4.7\times10^{-6}$, $\tau_{c(AQH\cdot)} = 1.0$ ps, and $k_T = 5\times10^4$ s^{-1}, respectively.

thenyl radicals,[9b] may be due to slow recombination. The RP lifetime of AQ steeply increased from 1.6 μs at 0 T to 6.0 μs at 2 T with the magnetic field, and then slowly decreased to 3.8 μs at 13 T. The maximum RP lifetime was obtained at around 2 T. The RP lifetime at 2 T increased to ca. 370% of that at 0 T, and the lifetime at 13 T decreased to ca. 60% of that at 2 T. The increment ($\Delta k_{3—13T}$) in the decay rates was 9.4×10^4 s^{-1} (Table 2), which was calculated from the lifetimes at 3.1 and 13 T and showed the magnitude of the δg interaction, as will be described later.

Similar reversals in the lifetime were observed in AQH··*n* in Brij35, and their maximum lifetimes also appeared at around 2 T (Fig. 4). Similarly, the RP lifetimes at 2 T increased up to > 370% of the lifetimes at 0 T, and those at 13 T lessened to ca. 60% of the respective maximum lifetimes at 2 T. The similar extent of increments, $\Delta k_{3—13T}$ ($(7.8—9.8)\times10^4$ s^{-1}), were obtained in all AQH··*n* as well as in AQH· (Table 2).

In each magnetic field of 0.5, 1.3, 2, 3.1, 5.7, 10, and 13 T listed in Table 1, the RP lifetimes of AQ-*n* in Brij35 showed the dependence of the methylene chain length (*n*), in which they became long when *n* increased. For example, the RP lifetimes at 1.3 T were 5.6 μs (AQH··2), 5.8 μs (AQH··3), 6.8 μs (AQH··4), 7.2 μs (AQH··6), and 7.1 μs (AQH··8), respectively.

Table 2. Increment ($\Delta k_{3—13T}$) in Observed RP Decay Rates (k_{RP}) as Increasing Magnetic Fields from 3.1 to 13 T[a)]

Quinone	Surfactant	$\Delta k_{3—13T}/10^4$ s^{-1}
AQ	Brij35	9.4
AQ	HDTCl	6.6
AQ	SDS	—[b)]
AQ-2	Brij35	7.8
AQ-3	Brij35	8.3
AQ-4	Brij35	9.5
AQ-6	Brij35	9.8
AQ-8	Brij35	7.9

a) Experimental error was about 10%. Data in Table 1 were used for the calculation. b) The value was not calculated accurately because of its very small increment compared with the experimental error.

HDTCl. The RP lifetimes in HDTCl were longer than in Brij35 above 0.5 T. A reversal in the MFD of the RP lifetimes was also observed. The lifetime of 1.5 μs at 0 T increased to 12 μs at 2 T and then decreased to 5.9 μs at 13 T. The maximum lifetime was detected around 2 T. The RP lifetime at 2 T increased to 800% of that at 0 T, and the lifetime at 13 T decreased to ca. 50% of that at 2 T. The increment ($\Delta k_{3—13T}$) in the decay rates from 3.1 to 13 T was 6.6×10^4 s^{-1} (Table 2). This value was smaller than that (9.4×10^4 s^{-1}) in Brij35.

SDS. The RP lifetime at 0 T in SDS was not obtained, because of the low AQH· generation, as suggested by the long ^{3}AQ* lifetime (τ_T = 335 ns), compared with the other surfactants (τ_T = 154 ns in Brij35 and 126 ns in HDTCl). Therefore, the RP lifetimes were measured above 0.1 T. The lifetime of 1.5 μs at 0.15 T increased to 4.0 μs at 2 T and showed no detectable change above 2 T within the experimental accuracy. No reversal in the MFD of the lifetime appeared, which was different from the cases of Brij35 and HDTCl. The lifetimes were shorter than, or equal to, those obtained in Brij35 and HDTCl in all magnetic fields.

Discussion

Mechanism for MFEs. Scheme 1 shows energy diagrams of RP in both the absence and presence of a high magnetic field larger than 0.1 T when the exchange interaction is negligibly small. In the absence of a magnetic field, ^{3}RP decays rapidly via Eqs. 4 and 7 ($(T_{\pm1}, T_0)\longrightarrow S\longrightarrow$ (recombination products) pathways in Scheme 1). In a field higher than 0.1 T, where the three substates (T_{+1}, T_0, and T_{-1}) are energetically separated, there are two well-known mechanisms for MFEs. They are mechanisms of (1) Δg and (2) SLR. The former causes a decrease in the RP life-

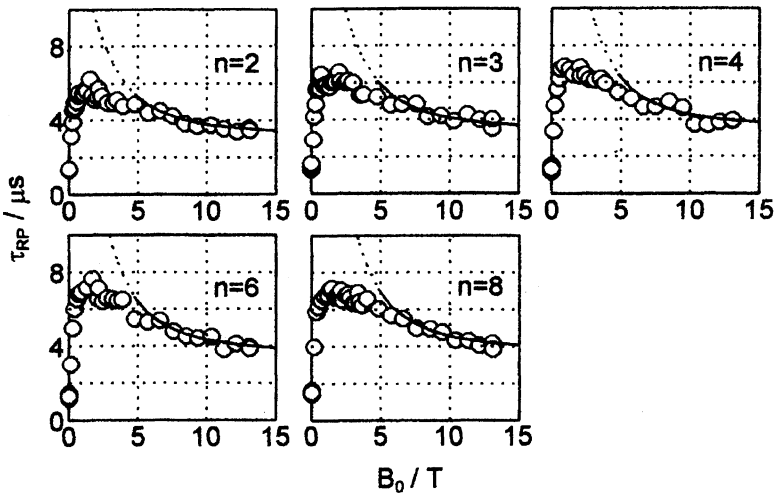

Fig. 4. Observed MFD plots of RP lifetimes of [AQH·−*n*+R·] (*n* = 2, 3, 4, 6, and 8) generated in Brij35. Solid lines were calculated using Eq. 11 with $(g:g)_{(AQH\cdot)} = 4.7\times10^{-6}$, $\tau_{c(AQH\cdot)}$ = 1.0 ps, $(g:g)_{(R\cdot)} = 5.3\times10^{-6}$, $\tau_{c(R\cdot)}$ = 1.1 ps, $k_T = 8\times10^4$ s^{-1} (*n* = 2), 6×10^4 s^{-1} (*n* = 3), 5×10^4 s^{-1} (*n* = 4), 4.6×10^4 s^{-1} (*n* = 6), and 3.5×10^4 s^{-1} (*n* = 8).

time with the magnetic field, while the latter causes both an increase and a decrease.

In the former mechanism, the parameter Δg is the difference in the isotropic g-values of the component radicals of RP. From the Δg value (0.0013) between AQH· and R· ($g_{(AQH\cdot)} = 2.0044$ and $g_{(MeC\cdot HOEt)} = 2.0031$),[16,17] the Δg-induced ISC ($T_0 \rightarrow S$) rate constant at 10 T can be estimated to be 5.7×10^8 s^{-1}. Since the experimental RP decay rate (2.3×10^5 s^{-1}) of AQ-8 at 10 T, which is calculated from its lifetime (4.3 μs), is much smaller than the calculated ISC rate (5.7×10^8 s^{-1}) by three orders of magnitude, the Δg-induced $T_0 \rightarrow S$ ISC is not a rate-determining step of the RP decay at a high magnetic field. Therefore, the Δg mechanism seems to be inadequate for explaining the decrease in the RP lifetime at a high magnetic field (> 2 T).

In the latter mechanism, if the initially populated state of RP is a triplet, the RPs populated in the S and T_0 states cannot proceed to the substates $T_{\pm1}$ because of the fast process of $T_0 \longrightarrow S \longrightarrow$recombination products. Therefore, the RP deactivation at a high magnetic field (> 0.1 T) can be assumed to be controlled mainly by the $T_{\pm1} \longleftrightarrow T_0$ and $T_{\pm1} \longleftrightarrow S$ pathways. In the SLR mechanism for RP, in general, the $T_{\pm1} \leftrightarrow T_0$ and $T_{\pm1} \leftrightarrow S$ transitions are considered to be modulated by three interactions: the δhf and δg interactions in each component radical, and the inter-radical dd interaction in RP.

Thus, the observed decay rate k_{RP} of RP composed of radicals AQH· and R· is expressed by[4b,9f,9h]

$$k_{RP} = 1/\tau_{RP} = (1/2)\{k(\text{AQH}\cdot : \delta\text{hf},\delta\text{g}) + k(\text{R}\cdot : \delta\text{hf},\delta\text{g})\} + k(\text{dd}) + k_T, \quad (9)$$

where k(AQH· : δhf,δg) and k(R· : δhf,δg) are the SLR rate constants governed by the δhf and δg interactions in each component radical and k(dd) is an SLR rate constant determined by the dd interaction in RP. The last term k_T is the rate constant for the direct disappearance from the ^{3}RP sublevels, which consists of the magnetic-field-independent escape (Eq. 5) and SO-induced ISC[15] (Eq. 6) processes. By using explicit expressions for the δhf, δg, and dd interactions, Eq. 9 is rewritten as a function of the magnetic field (B_0):[9h,18,19]

$$\begin{aligned} k_{RP} = 1/\tau_{RP} &= (1/2)\{k(\text{AQH}\cdot : \delta\text{hf},\delta\text{g}) + k(\text{R}\cdot : \delta\text{hf},\delta\text{g})\} \\ &\quad + k(\text{dd}) + k_T \\ &= (1/2)[\{(1/5)(\beta/\hbar)^2(g : g)_{(AQH\cdot)}B_0^2 \\ &\quad + \gamma^2 H_{loc(AQH\cdot)}^2\}\tau_{c(AQH\cdot)}/(1+\gamma^2B_0^2\tau_{c(AQH\cdot)}^2) \\ &\quad + \{(1/5)(\beta/\hbar)^2(g : g)_{(R\cdot)}B_0^2 \\ &\quad + \gamma^2 H_{loc(R\cdot)}^2\}\tau_{c(R\cdot)}/(1+\gamma^2B_0^2\tau_{c(R\cdot)}^2)] \\ &\quad + \gamma^2 H_{dd}^2\tau_c'/(1+\gamma^2B_0^2\tau_c'^2) + k_T, \end{aligned} \quad (10)$$

where β is the Bohr magneton, $\hbar$ is Plank's constant divided by 2π, B_0 is the external magnetic field, and γ is the magnetogyric ratio of an electron on AQH· and R· and is assumed to be equal to a free electron. The parameters τ_c and τ_c' are the rotational correlation times of spin tumbling for the δhf and δg interactions of AQH· and R· and for the dd interaction between the two radicals, respectively. The parameter $(g : g)$ is the inner product of the anisotropic g tensor. The parameters H_{loc} and H_{dd} are local magnetic fields due to the δhf and dd interactions, respectively.

According to the SLR model for MFE,[18,19] the RP lifetime determined by SLR due to the δhf and dd interactions increases with the magnetic field, whereas the lifetime determined by SLR due to the δg interaction decreases with the magnetic field. Therefore, the MFD curves in Figs. 3 and 4 were classified into two regions: 0.1—2 T (MFE predominantly due to the δhf and dd interactions) and 3—13 T (MFE mostly due to the δg interaction).

MFEs in 3—13 T. In B_0 = 3—13 T, a decrease in the RP lifetime due to the δg interaction was observed for AQ in Brij35 and HDTCl (Fig. 3) and AQ-n in Brij35 (Fig. 4). At 13 T the lifetimes of AQ and AQ-n in Brij35 decreased to ca. 60% of their maximum lifetimes. The lifetime of AQ in HDTCl decreased to ca. 50% of its maximum lifetime. Whereas the δhf and dd interactions decelerating SLR are still active in 0.1—2 T, those interactions in 3—13 T can be neglected because their contributions to the lifetime reduce as $1/(1+\gamma^2B_0^2\tau_c^2)$, as shown in Eq. 10.

Neglecting the terms for the δhf and dd interactions, Eq. 10 can be rewritten as

$$\begin{aligned} k_{RP} = 1/\tau_{RP} &= (1/2)\{k(\text{AQH}\cdot : \delta\text{g}) + k(\text{R}\cdot : \delta\text{g})\} + k_T \\ &= (1/2)[\{(1/5)(\beta/\hbar)^2(g : g)_{(AQH\cdot)}B_0^2\}\tau_{c(AQH\cdot)} \\ &\quad /(1+\gamma^2B_0^2\tau_{c(AQH\cdot)}^2) \\ &\quad + \{(1/5)(\beta/\hbar)^2(g : g)_{(R\cdot)}B_0^2\}\tau_{c(R\cdot)} \\ &\quad /(1+\gamma^2B_0^2\tau_{c(R\cdot)}^2)] + k_T \end{aligned} \quad (11)$$

The increments ($\Delta k_{3\text{—}13T}$) in the decay rates from 3.1 to 13 T, which were calculated from their lifetimes, were $(7.8\text{—}9.8)\times10^4$ s^{-1} in AQ and AQ-n in Brij35 and 6.6×10^4 s^{-1} in AQ in HDTCl. The increment in AQ in HDTCl was smaller than that (9.4×10^4 s^{-1}) in AQ in Brij35. To understand these results, MFD of the RP lifetimes of BP in HDTCl should be used as a reference, since it showed no significant reversal in the lifetime above 4 T.[9g] In fact, $\Delta k_{3\text{—}13T}$ of 0.64×10^4 s^{-1} in BP in HDTCl was negligibly small, compared with the results obtained in this study. Therefore, these values may be categorized into three regions:

$$\begin{aligned} &\text{AQ and AQ-}n\text{ in Brij35 } ((7.8\text{—}9.8)\times10^4\text{ s}^{-1}) \\ &> \text{AQ in HDTCl } (6.6\times10^4\text{ s}^{-1}) \\ &\gg \text{BP in HDTCl } (0.64\times10^4\text{ s}^{-1}). \end{aligned} \quad (12)$$

The relation among the three regions directly means the relation in the magnitude of the δg interactions of these RPs. In fact, the experimentally-obtained RP lifetimes in 3—13 T were arranged as AQ in Brij35 < AQ in HDTCl < BP in HDTCl, where the shorter lifetime means a stronger δg interaction.

In SDS, on the other hand, the RP lifetime showed no detectable decrease above 2 T within the experimental error. This fact means that the lifetime is determined by the mag-

netic-field-independent processes, such as the escape (Eq. 5) and SO-induced ISC (Eq. 6), and that the contribution of δg interaction is negligibly small above 2 T. Although the reason why the RP decay in SDS is determined by the magnetic-field-independent processes is obscure at present, the following speculation may be conceivable: BP is known to dissolve in the Stern phase, which is the space between the hydrophilic ($SO_4^-Na^+$) and hydrophobic ($CH_3(CH_2)_{11}$) parts of SDS. From a structural similarity to BP, AQ is also considered to dissolve in the Stern phase, probably predicting that the escape rate of the generated AQH· from the micelle is affected by a spatial hindrance around hydrophilic functional groups ($SO_4^-Na^+$ in SDS, $N^+(CH_3)_3Cl^-$ in HDTCl, and $(OCH_2CH_2)_{23}OH$ in Brij35) of the surfactants. The two bulky head groups ($N^+(CH_3)_3Cl^-$ in HDTCl and $(OCH_2CH_2)_{23}OH$ in Brij35) could play the role of a cover on the micelle to inhibit the escape of AQH· from the micelle. However, the relatively small head group ($SO_4^-Na^+$) in SDS hardly seems to inhibit the escape, compared with those in HDTCl and Brij35.

Estimation of $(g:g)_{(AQH\cdot)}$ and $\tau_{c(AQH\cdot)}$ of AQH·. To determine either AQH· or R· of HDTCl as an important origin of the δg interaction, MFD of the RP lifetime of AQ in HDTCl should be compared with that of BP in HDTCl. Equation 12 indicates that the magnitude ($I_{\delta g}(X)$) of the δg interaction of a radical X in HDTCl is $I_{\delta g}$(AQH· and R·) ≫ $I_{\delta g}$(BPH· and R·) > $I_{\delta g}$(R·). Since $\Delta k_{3\text{—}13T}$ for BP in HDTCl is 10-times smaller than $\Delta k_{3\text{—}13T}$ for AQ in HDTCl, as shown in Eq. 12, $I_{\delta g}$(R·) is interpreted to be *less than* 10-times $I_{\delta g}$(AQH· and R·). Therefore, the magnitude of the δg interaction of R· of HDTCl can be assumed to be negligibly small, compared to that of AQH·; that is, the reversal in the RP lifetime in the high magnetic field can be assumed to be due to only the δg interaction of AQH·.

Thus, Eq. 11 for AQ in HDTCl can be simplified as

$$k_{RP(HDTCl)} = 1/\tau_{RP(HDTCl)} = (1/2)\{k(AQH\cdot : \delta g)\} + k_{T(HDTCl)}$$
$$= (1/2)[\{(1/5)(\beta/\hbar)^2(g:g)_{(AQH\cdot)}B_0^2\}\tau_{c(AQH\cdot)}/(1+\gamma^2B_0^2\tau_{c(AQH\cdot)}^2)] + k_{T(HDTCl)}. \quad (13)$$

Hence,

$$1/(k_{RP(HDTCl)} - k_{T(HDTCl)}) = 1/(1/\tau_{RP(HDTCl)} - k_{T(HDTCl)})$$
$$= 2\{\gamma^2\tau_{c(AQH\cdot)} + 1/(\tau_{c(AQH\cdot)}B_0^2)\}/\{(1/5)(\beta/\hbar)^2(g:g)_{(AQH\cdot)}\}. \quad (14)$$

This equation shows that the left-hand term is linearly proportional to $1/B_0^2$, and that the parameters of $(g:g)_{(AQH\cdot)}$ and $\tau_{c(AQH\cdot)}$ for the δg interaction of AQH· can be evaluated from the slope and intercept of the plot when the left-hand term $1/(1/\tau_{RP} - k_{T(HDTCl)})$ is plotted against $1/B_0^2$. Those parameters are estimated according to the following relation of $(g:g)_{(AQH\cdot)} = 2\gamma\{(\text{slope})\times(\text{intercept})\}^{-0.5}/\{(1/5)(\beta/\hbar)^2\}$ and $\tau_{c(AQH\cdot)} = \{(\text{intercept})/(\text{slope})\}^{0.5}/\gamma$. To avoid contributions of the δhf and dd interactions as much as possible, the RP lifetimes measured only above 4.4 T were used in Eq. 14 (Fig. 5a). The parameter $k_{T(HDTCl)}$ was varied so that the plot represented a linear relation. The parameter $k_{T(HDTCl)}$ used

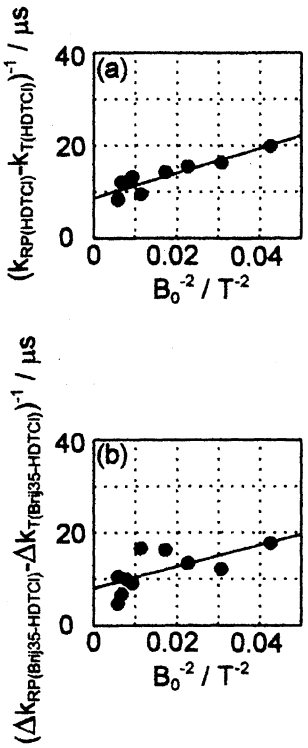

Fig. 5. (a) The plot of $1/(k_{RP(HDTCl)} - k_{T(HDTCl)})$ versus $1/B_0^2$ according to Eq. 14. (b) The plots of $1/(\Delta k_{RP(Brij35-HDTCl)} - \Delta k_{T(Brij35-HDTCl)})$ versus $1/B_0^2$ according to Eq. 15.

was $(5\pm0.5)\times10^4$ s^{-1}. The slope and intercept for AQH· in HDTCl were calculated to be 270±45 μs T^2 and 8.7±1.7 μs, respectively, by means of a least-squares fitting with Eq. 14 (Fig. 5a). From the fitting, $(g:g)_{(AQH\cdot)}$ and $\tau_{c(AQH\cdot)}$ for AQH· were calculated to be $(4.7\pm0.6)\times10^{-6}$ and 1.0±0.1 ps, respectively (Table 3). The solid curve in Fig. 3, calculated with the obtained $(g:g)_{(AQH\cdot)}$ and $\tau_{c(AQH\cdot)}$, is well superimposed on the experimental MFD plot above 5 T, where the δg interaction plays an important role.

Estimation of $(g:g)_{(R\cdot)}$ and $\tau_{c(R\cdot)}$ of R· of Brij35. The value $(9.4\times10^4$ $s^{-1})$ of $\Delta k_{3\text{—}13T}$ for AQ in Brij35 in Table 2 was larger than that $(6.6\times10^4$ $s^{-1})$ for AQ in HDTCl. This result suggests that the δg interaction due to R· of Brij35 plays a more important role than that of HDTCl based on the assumption that the contributions of the δg interaction of AQH· are almost the same between Brij35 and HDTCl. Therefore, the shorter RP lifetimes in Brij35, compared with

Table 3. $(g:g)$ and τ_c Obtained for the δg Interaction of Component Radicals and k_T

Component radical	Surfactant	$(g:g)/10^{-6}$	τ_c/ps	$k_T/10^4$ s^{-1}
AQH·	HDTCl	4.7±0.6	1.0±0.1	5±0.5
R·	Brij35	5.3±1.5	1.1±0.3	5±1
AQH·-2	Brij35	—	—	8±1
AQH·-3	Brij35	—	—	6±1
AQH·-4	Brij35	—	—	5±1
AQH·-6	Brij35	—	—	4.6±0.8
AQH·-8	Brij35	—	—	3.5±0.7

in HDTCl at each magnetic field, are recognized as being the δg interaction enhanced by R· of Brij35. At each magnetic field above 3 T, as shown in Table 1, the increments (Δk_{RP}) in the observed RP decay rates between Brij35 and HDTCl are expressed as the difference between $k_{RP(Brij35)}$ (Eq. 11) and $k_{RP(HDTCl)}$ (Eq. 13). The term for the δg interaction due to AQH· is canceled by subtraction:

$$\begin{aligned}\Delta k_{RP(Brij35-HDTCl)} &= k_{RP(Brij35)} - k_{RP(HDTCl)} \\ &= (1/2)\{k(R\cdot : \delta g)\} + k_{T(Brij35)} - k_{T(HDTCl)} \\ &= (1/2)[\{(1/5)(\beta/\hbar)^2(g : g)_{(R\cdot)}B_0^2\}\tau_{c(R\cdot)} \\ &\quad /(1+\gamma^2B_0^2\tau_{c(R\cdot)}^2)] + \Delta k_{T(Brij35-HDTCl)}, \end{aligned} \quad (15)$$

where $k_{T(Brij35)}$ and $k_{T(HDTCl)}$ denote the magnetic-field-independent terms expressed in Eqs. 5 and 6, and $\Delta k_{T(Brij35-HDTCl)}$ is the difference between them. Therefore, according to the same procedure as shown in Eqs. 13 and 14, the parameters of $\tau_{c(R\cdot)}$ and $(g : g)_{(R\cdot)}$ for the δg interaction due to R· of Brij35 are evaluated from the plot of $1/(\Delta k_{RP(Brij35-HDTCl)} - \Delta k_{T(Brij35-HDTCl)})$ versus $1/B_0^2$ (Fig. 5b). The parameter $\Delta k_{T(Brij35-HDTCl)}$ was varied so that the plot represented a linear relation. The obtained parameter $k_{T(Brij35)}$ was $(5\pm1)\times10^4$ s^{-1}, using the already obtained $k_{T(HDTCl)} = 5\times10^4$ s^{-1}. From the obtained slope and intercept, $(g : g)_{(R\cdot)}$ and $\tau_{c(R\cdot)}$ for R· of Brij35 were calculated to be $(5.3\pm1.6)\times10^{-6}$ and 1.1±0.3 ps, respectively. The solid curve in Fig. 3, calculated by Eq. 11 and the obtained parameters of $(g : g)_{(AQH\cdot)} = 4.7\times10^{-6}$, $\tau_{c(AQH\cdot)} = 1.0$ ps, $(g : g)_{(R\cdot)} = 5.3\times10^{-6}$, $\tau_{c(R\cdot)} = 1.1$ ps, and $k_T = 5\times10^4$ s^{-1} for AQ in Brij35, well reproduced the experimental MFD plot above 4.8 T, which proves the δg interactions due to both AQH· and R· of Brij35.

In summary, the key radicals which determine the magnitude of the δg interaction, that is, the RP lifetime, could be denoted as

(I) AQH· for AQ in HDTCl,

(II) AQH· and R· for AQ in Brij35.

As for the MFDs of AQ-*n* in Brij35, a good reproduction was obtained using the same parameters ($(g : g)_{(AQH\cdot)} = 4.7\times10^{-6}$, $\tau_{c(AQH\cdot)} = 1.0$ ps, $(g : g)_{(R\cdot)} = 5.3\times10^{-6}$, $\tau_{c(R\cdot)} = 1.1$ ps) for AQ in Brij35 (Fig. 4). The k_T parameters used were $(8\pm1)\times10^4$ s^{-1} (AQH·-2), $(6\pm1)\times10^4$ s^{-1} (AQH·-3), $(5\pm1)\times10^4$ s^{-1} (AQH·-4), $(4.6\pm0.8)\times10^4$ s^{-1} (AQH·-6), and $(3.5\pm0.7)\times10^4$ s^{-1} (AQH·-8), respectively. These values (Table 3) decreased when the length (*n*) of the methylene chain became long. Since k_T seems to be predominantly determined by the escape process (Eq. 5), as will be described later, the obtained trend of a smaller k_T in a larger *n* is apprehensible.

Discussion for $(g : g)$ and τ_c Obtained. As for $(g : g)$, the value $((4.7\pm0.6)\times10^{-6})$ for AQH· is similar to both the value (10.6×10^{-6}) for AQH· estimated using a *g* tensor ($g_1 = 2.0067$, $g_2 = 2.0044$, and $g_3 = 2.0021$) supposed[9b] and the experimental values $((7.69—9.36)\times10^{-6})$ so far reported for structurally similar benzosemiquinone-alkali metal ion (Li^+, Na^+, and K^+) pairs.[20a,20b] This similarity in $(g : g)$ suggests the validity of this kind of analysis (Eqs. 11, 12, 13, 14, and 15). The large $(g : g)$ value $((4.7\pm0.6)\times10^{-6})$ for AQH·, compared with that (0.447×10^{-6}) calculated from a *g* tensor ($g_1 = 2.0035$, $g_2 = 2.0033$, and $g_3 = 2.0026$) for an alkyl radical of HC·$(CO_2H)_2$,[20c] is considered to arise from the spin population on an oxygen atom of a phenoxyl radical moiety in AQH·. This may be supported by the large $(g : g)$ value (9.68×10^{-6}) for L-tyrosine-derived ·$OPhCH_2CH(NH_3^+)$-COO^- ($g_1 = 2.0023$, $g_2 = 2.0067$, and $g_3 = 2.0045$),[20d] which has the spin population on the oxygen.

On the other hand, the $(g : g)$ value $((5.3\pm1.6)\times10^{-6})$ for R· of Brij35 was occasionally obtained to be similar to that $((4.7\pm0.6)\times10^{-6})$ for AQH·. The reliability of this $(g : g)$ value for R· might be supported by the value (6.54×10^{-6}) based on a *g* tensor ($g_1 = 2.0053$, $g_2 = 2.0038$, and $g_3 = 2.0017$) for HC·(OH)(CO_2H), which has a similar structure from the point of view that an oxygen atom links up with a carbon radical.[20c] The large value for R· of Brij35 also seems to be due to some extent of the spin population on the oxygen atom.

The compatibility of the experimentally-obtained $(g : g)$ values for AQH· and R· of Brij35 with those in the literature may allow us to accept the already above-mentioned assumptions used in estimating $(g : g)$ and τ_c: (1) the magnitude ($I_{\delta g}(R\cdot)$) of the δg interaction of R· of HDTCl is negligibly small in comparison with $I_{\delta g}(AQH\cdot)$, which was used in estimating AQH·, and (2) the contribution of the δg interaction of AQH· between Brij35 and HDTCl is almost the same, despite the different surfactants, which was used in estimating R· of Brij35. The key for estimating $(g : g)$ and τ_c is assumption (1); that is, $I_{\delta g}(R\cdot) \fallingdotseq 0$ in HDTCl. This assumption (1) is based on the fact in HDTCl that $I_{\delta g}(R\cdot)$ is *less than* 10-times $I_{\delta g}$(AQH· and R·) in the relation of $I_{\delta g}$(AQH· and R·) $\gg I_{\delta g}$(BPH· and R·) $> I_{\delta g}(R\cdot)$, as already shown in Eq. 12.

As for τ_c, the values of 1.0±0.1 ps for AQH· and 1.1±0.3 ps for R· of Brij35 are both exceptionally small compared with that (59 ps) calculated using the Stokes–Einstein–Debye (SED) equation, which is often used to estimate τ_c for the radical motion as a whole. Obviously, these small values cannot be assigned to the radical motion as a whole. These seem to be attributable to fast local motions present inside the radical molecules. In our previous studies,[9b,9d—9g,10] similarly drastic reversals in the MFDs of lifetimes of BRs linked by flexible methylene chains were measured in homogeneous solutions. In the most drastic decrease among them, the BR lifetime in an α-cyclodextrin inclusion complex of phenothiazine–viologen chain-linked compound lessened to about 30% of the maximum lifetime.[9f] From an analysis of MFD, an extremely small τ_c (1 ps) was obtained. As an environmental character surrounding the component radicals, the viscosity of a homogeneous solution should be very different from that of a micellar solution. Therefore, if the δg interaction would be determined by the environment and radical motion as a whole, τ_c must be greatly different mutually between them; that is, τ_c must depend on the solution and the overall size of the radical molecule. The similarity in τ_c of the apparently different environment and structurally-different

radicals (AQH· and R· of Brij35) might imply the responsibility not due to the radical motion as a whole, but to fast local motions probably commonly present inside the radical molecules with such a small correlation time. Although we cannot exactly state the assignment of the fast local motions at present, local motions similar to a torsional vibration around C–N bonds linking an alkane to pyridyl and/or phenothiazine rings, suggested in the phenothiazine-viologen inclusion system,[9f] might be responsible for the small τ_c.

MFEs in 0.1—2 T. Since the increase in the lifetime was detected in this low magnetic field region of $B_0 = 0.1$—2 T, the δhf and dd interactions due to AQH· and R· should be taken into consideration. The δg interaction can be ignored, since its contribution is negligibly small in this region because of its B_0^2 dependence, as shown in Eq. 11. Therefore, by subtracting Eq. 11 from Eq. 10, the RP decay rate constant Δk_{RP} in this low magnetic field region is expressed as

$$\begin{aligned}\Delta k_{RP} &= (k_{RP} \text{ in Eq. 10}) - (k_{RP} \text{ in Eq. 11})\\ &= (1/2)\{k(\text{AQH}\cdot : \delta\text{hf}) + k(\text{R}\cdot : \delta\text{hf})\} + k(\text{dd})\\ &= (1/2)[\gamma^2 H_{\text{loc(AQH}\cdot)}^2 \tau_{c(\text{AQH}\cdot)}/(1+\gamma^2 B_0^2 \tau_{c(\text{AQH}\cdot)}^2)\\ &\quad + \gamma^2 H_{\text{loc(R}\cdot)}^2 \tau_{c(\text{R}\cdot)}/(1+\gamma^2 B_0^2 \tau_{c(\text{R}\cdot)}^2)]\\ &\quad + \gamma^2 H_{dd}^2 \tau_c'/(1+\gamma^2 B_0^2 \tau_c'^2). \end{aligned} \quad (16)$$

Since there are unknown parameters, such as H_{loc}, H_{dd}, τ_c, and τ_c' in Eq. 16, it is difficult to distinguish the δhf interaction quantitatively (H_{loc} and τ_c) from the dd interaction (H_{dd} and τ_c') without experiments, such as concerning the magnetic isotope effects on the MFE.[4a,8a,8b,9h,10,21,22] To evaluate the δhf interaction independently in distinction from the dd interaction, the lifetime of a naturally-abundant RP should be compared with that of a magnetic-isotope (^{2}H, ^{13}C, ^{15}N, and so on)-substituted RP. These magnetic isotopes have nuclear spins to enlarge only H_{loc} for the δhf interaction without affecting any other parameters in Eq. 10. In this work, therefore, the effective values of the local magnetic field (H_{eff}) and rotational correlation time (τ_{eff}) averaged for both the δhf (H_{loc} and τ_c) and dd (H_{dd} and τ_c') interactions were tentatively evaluated. Although the two correlation times of τ_c and τ_c' should be essentially different from each other, $\tau_c = \tau_c' = \tau_{eff}$ was assumed because of no practical information on the values at present. However, this assumption is sufficient to elucidate which radical between AQH· and R· in the micelle is predominantly related to determining the RP lifetime, as will be described later. Since the terms of the δhf and dd interactions in Eq. 16 are shown by the same expression on the local magnetic field (H_{loc} and H_{dd}), the rotational correlation time (τ_c and τ_c'), and the external magnetic field (B_0), Eq. 16 is rewritten for AQH· in Brij35 as

$$\begin{aligned}\Delta k_{RP(\text{Brij35})} &= (k_{RP(\text{Brij35})} \text{ in Eq. 10}) - (k_{RP(\text{Brij35})} \text{ in Eq. 11})\\ &= \gamma^2 H_{eff}^2 \tau_{eff}/(1+\gamma^2 B_0^2 \tau_{eff}^2). \end{aligned} \quad (17)$$

From the reciprocal of Eq. 17, the following equation is obtained:

$$1/\Delta k_{RP(\text{Brij35})} = 1/(\gamma^2 {H_{eff}}^2 \tau_{eff}) + {B_0}^2 \tau_{eff}/{H_{eff}}^2. \quad (18)$$

Equation 18 denotes that the effective mean values of H_{eff} and τ_{eff} can be obtained analytically from the values of the intercept ($1/(\gamma^2 H_{eff}^2 \tau_{eff})$) and the slope ($\tau_{eff}/H_{eff}^2$) when the left-hand term in Eq. 18 is plotted against B_0^2. Figure 6a depicts a plot of Eq. 18 for AQ in Brij35. To calculate the term of ($k_{RP(\text{Brij35})}$ in Eq. 11) in Eq. 17, the already obtained values ($(g:g)_{(\text{AQH}\cdot)} = 4.7\times10^{-6}$, $\tau_{c(\text{AQH}\cdot)} = 1.0$ ps, $(g:g)_{(\text{R}\cdot)} = 5.3\times10^{-6}$, $\tau_{c(\text{R}\cdot)} = 1.1$ ps, and $k_T = 5\times10^4$ s^{-1}) were used for the δg interaction and k_T. The effective mean values were obtained to be H_{eff}=1.4±0.1 mT and τ_{eff} = 2.0±0.3 ps using the relationships of $H_{eff}=\{\gamma^2(\text{slope})\times(\text{intercept})\}^{-0.25}$ and $\tau_{eff} = \{(\text{slope})/(\text{intercept})\}^{0.5}/\gamma$. Table 4 lists the values of H_{eff} and τ_{eff} with the cases of AQ-*n* in Brij35. All of the AQ derivatives in Brij35 showed almost the same values in H_{eff} (1.4 mT) and τ_{eff} (2 ps), respectively.

For AQ in HDTCl, the following equation was used in place of Eq. 17, since the δg interaction due to R· can be ignored (as discussed above):

$$\begin{aligned}\Delta k_{RP(\text{HDTCl})} &= (k_{RP(\text{HDTCl})} \text{ in Eq. 10}) - (k_{RP(\text{HDTCl})} \text{ in Eq. 13})\\ &= \gamma^2 H_{eff}^2 \tau_{eff}/(1+\gamma^2 B_0^2 \tau_{eff}^2). \end{aligned} \quad (19)$$

According to the manner expressed in Eq. 18, the effective mean values of H_{eff} and τ_{eff} were obtained to be H_{eff}= 0.86±0.18 mT and τ_{eff} = 5.5±2.4 ps from the plot (Fig. 6b).

In AQ in SDS, the lifetime increased below 2 T and then showed no detectable change above 2 T within the experimental error, as already described. This fact means that the lifetimes are determined by SLR due to the δhf and dd interactions below 2 T, while by the magnetic-field-independent processes above 2 T, indicating that the contribution

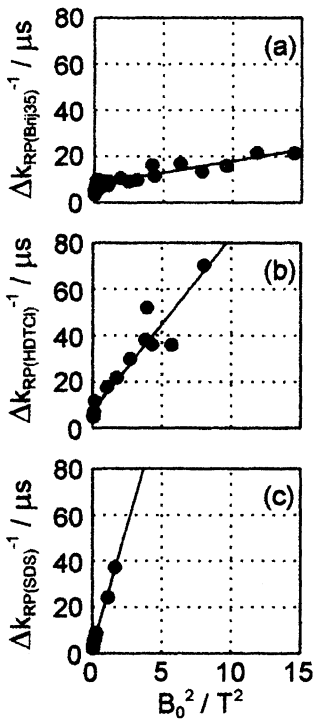

Fig. 6. Plots of $1/\Delta k_{RP}$ versus B_0^2 for estimating the effective parameters of H_{eff} and τ_{eff} according to Eq. 18 for Brij35 (a), Eq. 19 for HDTCl (b), and Eq. 20 for SDS (c).

Table 4. Effective Mean Values of H_{eff} and τ_{eff} Obtained by Averaging Both the δhf and dd Interactions

Quinone or Ketone	Surfactant	H_{eff}/mT	τ_{eff}/ps	$k_T/10^4$ s^{-1}
AQ	Brij35	1.4±0.1	2.0±0.3	5±1[b]
AQ	HDTCl	0.86±0.18	5.5±2.4	5±0.5[b]
AQ	SDS	0.85±0.06	15±2	26.2±1.8
AQ-2	Brij35	1.4±0.1	1.7±0.2	8±1[b]
AQ-3	Brij35	1.4±0.1	2.1±0.2	6±1[b]
AQ-4	Brij35	1.3±0.1	1.9±0.4	5±1[b]
AQ-6	Brij35	1.3±0.1	2.2±0.5	4.6±0.8[b]
AQ-8	Brij35	1.4±0.1	2.4±0.4	3.5±0.7[b]
BP	SDS	0.99±0.23[a]	16±7.5[a]	17.2[a]

a) Obtained from Ref. 9a. b) Cited from Table 3.

of δg interaction is negligibly small above 2 T in comparison with that of the magnetic-field-independent processes. Assuming a negligibly small magnitude of the δg interaction for R· of SDS as well as HDTCl, an increment in k_{RP} due to the δg interaction of AQH· in SDS can be calculated according to $(1/2)\{k(\text{AQH}\cdot : \delta g)\}$ in Eq. 13. When $(g : g)_{(\text{AQH}\cdot)} = 4.7\times10^{-6}$ was taken from Table 3, the increments at 10 T were tentatively obtained to be 8.9×10^4 and 0.20×10^4 s^{-1} at $\tau_{c(\text{AQH}\cdot)} = 1$ and 59 ps, respectively, in which the latter τ_c (59 ps) was estimated by the SED equation. By adding directly to the experimental RP decay rate ($(4\ \mu s)^{-1}$) at 2 T (see Table 1), these values led to the RP lifetimes (2.9 and 4.0 μs at 10 T, respectively), including the estimated contribution of the δg interaction of AQH·. However, even if $\tau_{c(\text{AQH}\cdot)} = 1$ is correct for SDS, we unfortunately cannot mention any difference between them (the observed 4.0 μs at 2 T and calculated 2.9 μs at 10 T), because of our experimental accuracy, as shown in Fig. 3. This is the reason why the contribution of δg interaction was neglected above 2 T in SDS. Therefore, ignoring all of the δg interactions, Eq. 17 for AQ in SDS is expressed as

$$\Delta k_{RP(SDS)} = (k_{RP(SDS)} \text{ in Eq. 10}) - k_{T(SDS)} = \gamma^2 H_{eff}^2 \tau_{eff}/(1+\gamma^2 B_0^2 \tau_{eff}^2). \quad (20)$$

Here, the magnetic-field-independent k_T was obtained to be $(26.2\pm1.8)\times10^4$ s^{-1} from the mean value of the RP lifetimes measured between 2 and 13 T, as depicted in Fig. 3. According to the manner expressed in Eq. 18, the effective mean values of H_{eff} and τ_{eff} were obtained to be H_{eff}=0.85±0.06 mT and τ_{eff} = 15±2 ps from the plots (Fig. 6c).

As for H_{eff} and τ_{eff}, there was no difference among AQH· and AQH·-*n* in Brij35, and they were almost 1.4 mT and 2 ps, respectively. The values of H_{eff} and τ_{eff}, which resulted from analyzing the δhf and dd interactions inclusively, were interpreted qualitatively. Since theoretical estimations of the local magnetic fields (H_{loc}) due to the δhf interaction so far reported were successful,[9a,9h,23] the theoretical values of H_{loc} were also calculated in the same manner, as summarized in Table 5. From these values, an averaged H_{loc} for RP composed of AQH· and R· were obtained to be 0.66 mT using the relation $H_{loc} = \{(H_{loc} \text{ for AQH}\cdot)^2 + (H_{loc} \text{ for R}\cdot)^2\}^{0.5} = (0.16^2+0.64^2)^{0.5}$. This value is smaller than the experimentally obtained H_{eff}, and hence the difference between the theoretical H_{loc} and experimental H_{eff} might indicate a contribution of the dd interaction. On the other hand, even if H_{eff} is predominantly determined by the dd interaction, which is dependent on the distance between the two component radicals of RP, the constant H_{eff} in Brij35 is understandable because the distance in the intermolecularly generated RP seems to be almost constant. This is because the site where a radical is generated in AQ-*n* is a moiety of AQ, not the methylene chain. At present, therefore, which interaction predominantly governs H_{eff}, that is, the RP lifetime, is unclear. H_{eff} showed the micellar dependence of H_{eff} (AQ in SDS) = H_{eff} (AQ in HDTCl) = H_{eff} (BP in SDS) < H_{eff} (AQ in Brij35), which indicates that H_{eff} is the same as each other between the two structurally identical alkyl radicals in SDS and HDTCl in spite of the different solutes (AQ and BP) in them. Similarly, τ_{eff} showed micellar dependences of τ_{eff} (AQ in SDS) = τ_{eff} (BP in SDS) and of τ_{eff} (AQ in Brij35) < τ_{eff} (AQ in HDTCl) < τ_{eff} (AQ in SDS), which indicate that τ_{eff} is definitely dependent on the surfactants, despite the same solute (AQ). These dependences in H_{eff} and τ_{eff} clearly suggest that a key radical determining H_{eff} and τ_{eff} is R·, rather than AQH·, though it is obscure wether the main origin is the δhf or rotational and translational[24] dd interactions. Concerning the reliability of the experimentally obtained parameters listed in Tables 3 and 4, Fig. 7 shows good reproduction of the MFDs in the cases of AQ in the three surfactants.

Dependences of RP Lifetimes on Methylene Chain Length (*n*). In each magnetic field of 0.5, 1.3, 2, 3.1, 5.7, 10, and 13 T listed in Table 1, the RP lifetimes of AQ-*n* in Brij35 increased when *n* increased. For example, the RP lifetimes at 1.3 T are 5.6 μs (AQH·-2), 5.8 μs (AQH·-3), 6.8 μs (AQH·-4), 7.2 μs (AQH·-6), and 7.1 μs (AQH·-8), respectively. This increase in the RP lifetime may be explained in terms of a decrease in the escape rate of AQH·-*n* from the micelle (Eq. 5). Unfortunately, the escape rate could not be calculated using the results of Eq. 8, because of the obstructive coexistence of an absorption band due to recombination products at 400 nm, as already mentioned. However, the *n* dependence of k_T could be obtained experimentally in the above analysis in 3—13 T (Table 3). The k_T values for AQH·-*n* in Brij35 showed the *n* dependence to become small when *n* increased. Further, a difference $(1/\tau_{RP(\text{AQH}\cdot-2)} - 1/\tau_{RP(\text{AQH}\cdot-8)})$ in the observed RP decay rates between AQH·-2 and AQH·-8 in each magnetic field above 0.1 T showed no MFD within the experimental accuracy (Fig. 8). Since the parameters for the δhf, dd, and

Table 5. Theoretical Values of the Local Magnetic Field (H_{loc}) for the δhf Interaction

Component radical	H_{loc}/mT
AQH·	0.16
R· of SDS or HDTCl	0.64

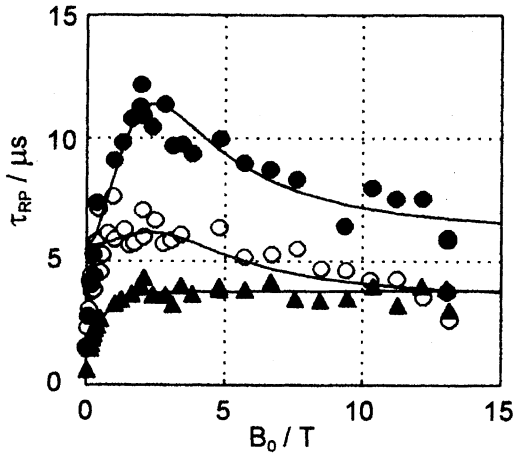

Fig. 7. Observed MFD plots of RP lifetimes of [AQH·+R·] generated in Brij35 (○), HDTCl (●), and SDS (▲). Solid lines were calculated using estimated values summarized in Tables 3 and 4.

δg interactions, except for k_T, should be equal each to each, the difference $(1/\tau_{RP(AQH\cdot-2)} - 1/\tau_{RP(AQH\cdot-8)})$, which corresponds to the difference in k_T between AQH·-2 and AQH·-8, should be constant, despite the magnetic field. Therefore, no MFD observed in the difference indicates that the magnetic-field-dependent interactions, such as the δhf, δg, and dd interactions, are not responsible for the increase in the RP lifetime when n increases. Since the micellar core is hydrophobic and the hydrophobicity in AQH·-n increases when n increases, we assume that a long methylene chain of AQH·-8 interacts strongly with the core, resulting in the smallest escape rate. A small escape rate in a large n leads to a small k_T, and hence a long RP lifetime. The result that the k_T values for AQH·-2, AQH·-3, AQH·-4, and AQH·-6 were greater than or equal to that for AQH· might be caused by the hydrophilicity of carbonyloxy groups absent from AQH· and/or by the enhanced SO-induced ISC rate due to the heavy atom of oxygen.

On the other hand, expecting observable differences in the magnetic-field-independent SO-induced ISC rates[15] among the RPs derived from AQ-n is difficult. As already described above, AQ-n in the micelle abstracts a hydrogen atom from a surfactant not from an intramolecular methylene chain, judging from the result that the *intramolecular* hydrogen abstraction rate in AQ-8 in Freon® 113 was very slow (30.4 μs).[14a] This intermolecular hydrogen abstraction implies almost constant distances between the component radicals (AQH·-n and R·) in RPs, directly showing almost the same magnitude of the SO interaction among them.

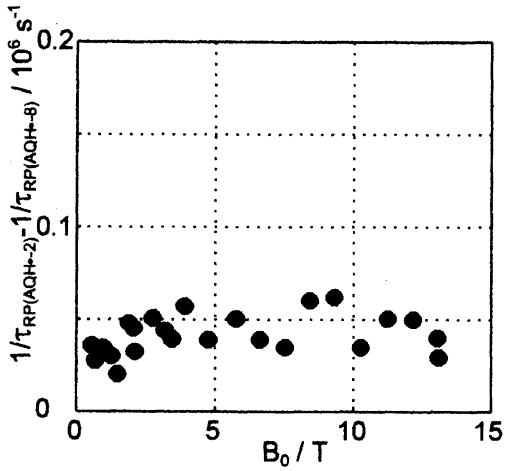

Fig. 8. MFD of a difference between observed RP decay rates of AQH·-2 and AQH·-8 in Brij35.

Summary

The RP lifetimes of AQ in Brij35, HDTCl, and SDS and those of AQ-n in Brij35 increased with increasing the magnetic field from 0 to about 2 T. The RP lifetimes of AQ in Brij35 and HDTCl drastically decreased in a magnetic field from 3 to 13 T, whereas the RP lifetimes of AQ in SDS were constant in the same range of the magnetic field. The drastic MFDs of the RP lifetimes were discussed based on the SLR mechanism. The increase in the RP lifetime in 0.1—2 T was interpreted by the δhf and dd interactions modulating SLR, while the decrease in 3—13 T in Brij35 and HDTCl was explained by the δg interaction. In comparison with MFD of the RP lifetimes of BP in HDTCl, the values of $(g:g)$ and τ_c for the δg interactions of the respective component radicals (AQH· and R· of Brij35) were first evaluated experimentally by means of this kind of experiment at room temperature using a high magnetic field, where the δg interaction is the main operation, though there have been many reports on the anisotropic g-values in a rigid matrix at low temperature. The $(g:g)$ values for AQH· and R· were relatively large, which was interpreted to be due to the large g-anisotropy in oxygen where the electron spin seems to partly populate. The exceptionally small τ_c values were considered to represent the importance of fast local motions present inside the component radicals.

We really thank Dr. M. Okazaki in National Industrial Research Institute of Nagoya in Japan for his invaluable discussion for the theory of SLR. This work was financially supported partly by Grants-in-Aid for Scientific Research (Nos. 07740502 and 09740434) from the Ministry of Education, Science, Sports and Culture.

References

1 N. J. Turro and B. Krautler, *Acc. Chem. Res.*, **13**, 369 (1980).

2 B. Brocklehurst, *Int. Rev. Phys. Chem.*, **4**, 279 (1985).

3 a) Yu. N. Molin, "Spin Polarization and Magnetic Effects in Radical Reactions," Elsevier, Amsterdam (1984). b) A. L. Buchachenko, *Chem. Rev.*, **95**, 2507 (1995).

4 a) U. E. Steiner and T. Ulrich, *Chem. Rev.*, **89**, 51 (1989). b) U. E. Steiner and H. -J. Wolff, "Photochemistry and Photophysics," CRC Press, Boca Raton (1991), Vol. iv, p. 1.

5 a) Y. Tanimoto, *Yakugaku Zasshi*, **109**, 505 (1989). b) Y. Tanimoto and Y. Fujiwara, *J. Synth. Org. Chem. Jpn.*, **53**, 413 (1995).

6 R. Nakagaki, Y. Tanimoto, and K. Mutai, *J. Phys. Org. Chem.*, **6**, 381 (1993).

7 H. Yonemura, H. Nakamura, and T. Matsuo, *Chem. Phys.*, **162**, 69 (1992).

8 a) Y. Sakaguchi, H. Hayashi, and S. Nagakura, *J. Phys. Chem.*, **86**, 3177 (1982). b) H. Hayashi and S. Nagakura, *Bull. Chem. Soc. Jpn.*, **57**, 322 (1984). c) H. Hayashi, "Photochemistry and Photophysics," CRC Press, Boca Raton (1990), Vol. i, Chap. 2. d) H. Hayashi and Y. Sakaguchi, "Lasers in Polymer Science and Technology: Application," CRC Press, Boca Raton (1990), Vol. 1, Chap. 1.

9 a) Y. Fujiwara, M. Mukai, T. Tamura, Y. Tanimoto, and M. Okazaki, *Chem. Phys. Lett.*, **213**, 89 (1993). b) M. Mukai, Y. Fujiwara, Y. Tanimoto, and M. Okazaki, *J. Phys. Chem.*, **97**, 12660 (1993). c) M. Mukai, H. Tanaka, Y. Fujiwara, and Y. Tanimoto, *Bull. Chem. Soc. Jpn.*, **67**, 3112 (1994). d) Y. Fujiwara, *Chem. Chem. Ind.*, **48**, 115 (1995). e) Y. Fujiwara, M. Mukai, and Y. Tanimoto, *Trans. IEE Jpn.*, **116-A**, 419 (1996). f) Y. Fujiwara, T. Aoki, K. Yoda, H. Cao, M. Mukai, T. Haino, Y. Fukazawa, Y. Tanimoto, H. Yonemura, T. Matsuo, and M. Okazaki, *Chem. Phys. Lett.*, **259**, 361 (1996). g) Y. Fujiwara, K. Yoda, T. Aoki, and Y. Tanimoto, *Chem. Lett.*, **1997**, 435. h) Y. Fujiwara, T. Aoki, T. Haino, Y. Fukazawa, Y. Tanimoto, R. Nakagaki, O. Takahira, and M. Okazaki, *J. Phys. Chem. A*, **101**, 6842 (1997). i) H. Cao, K. Miyata, T. Tamura, Y. Fujiwara, A. Katsuki, C. -H. Tung, and Y. Tanimoto, *J. Phys. Chem. A*, **101**, 407 (1997).

10 a) R. Nakagaki, Y. Fujiwara, and Y. Tanimoto, *Photochemistry*, **22**, 46 (1996). b) R. Nakagaki, M. Yamaoka, O. Takahira, K. Hiruta, Y. Fujiwara, and Y. Tanimoto, *J. Phys. Chem. A*, **101**, 556 (1997).

11 a) S. Ronco and G. Ferraudi, *Inorg. Chem.*, **29**, 3961 (1990). b) G. Ferraudi, *J. Phys. Chem.*, **97**, 11929 (1993).

12 P. Gilch, M. Linsenmann, W. Haas, and U. E. Steiner, *Chem. Phys. Lett.*, **254**, 384 (1996).

13 a) Y. Sakaguchi and H. Hayashi, *Chem. Lett.*, **1993**, 1183. b) Y. Nakamura, M. Igarashi, Y. Sakaguchi, and H. Hayashi, *Chem. Phys. Lett.*, **217**, 387 (1994). c) M. Igarashi, Q. -X. Meng, Y. Sakaguchi, and H. Hayashi, *Mol. Phys.*, **84**, 943 (1995). d) M. Wakasa, H. Hayashi, Y. Mikami, and T. Takada, *J. Phys. Chem.*, **99**, 13181 (1995). e) K. Nishizawa, Y. Sakaguchi, H. Hayashi, H. Abe, and G. Kido, *Chem. Phys. Lett.*, **267**, 501 (1997). f) M. Igarashi, Y. Sakaguchi, and H. Hayashi, *Chem. Phys. Lett.*, **243**, 545 (1995). g) M. Wakasa and H. Hayashi, *J. Phys. Chem.*, **100**, 15640 (1996). h) Y. Mori, Y. Sakaguchi, and H. Hayashi, *Chem. Phys. Lett.*, **286**, 446 (1998).

14 a) Y. Tanimoto, M. Uehara, M. Takashima, and M. Itoh, *Bull. Chem. Soc. Jpn.*, **61**, 3121 (1988). b) Y. Tanimoto, H. Udagawa, and M. Itoh, *J. Phys. Chem.*, **87**, 724 (1983). c) Y. Tanimoto, K. Shimizu, and M. Itoh, *Chem. Phys. Lett.*, **112**, 217 (1984). d) Y. Tanimoto, K. Shimizu, and M. Itoh, *J. Am. Chem. Soc.*, **106**, 7257 (1984).

15 a) L. Salem and C. Rowland, *Angew. Chem., Int. Ed. Engl.*, **11**, 92 (1972). b) G. L. Closs and O. D. Redwine, *J. Am. Chem. Soc.*, **107**, 6131 (1985). c) C. Doubleday, N. J. Turro, and J. -F. Wang, *Acc. Chem. Res.*, **22**, 199 (1989). d) I. V. Khudyakov, Y. A. Serebrennikov, and N. J. Turro, *Chem. Rev.*, **93**, 537 (1993). e) T. Ulrich, U. E. Steiner, and W. Schlenker, *Tetrahedron*, **42**, 6131 (1986). f) P. P. Levin and V. A. Kuzmin, *Chem. Phys.*, **162**, 79 (1992).

16 H. Haustein, K. Möbius, and K. P. Dinse, *Z. Naturforsch., A*, **24A**, 1768 (1969).

17 R. S. Davidson, F. A. Younis, and R. Wilson, *J. Chem. Soc., Chem. Commun.*, **1969**, 826.

18 A. Abragam, "The Principles of Nuclear Magnetism," Clarendon Press, Oxford (1961), Chap. 8.

19 A. Carrington and A. D. McLachlan, "Introduction to Magnetic Resonance with Application to Chemistry and Chemical Physics," Harper and Row, New York (1967), Chap. 11.

20 a) B. J. Hales, *J. Am. Chem. Soc.*, **97**, 5993 (1975). b) B. J. Hales, *J. Am. Chem. Soc.*, **98**, 7350 (1976). c) J. R. Morton, *Chem. Revs.*, **64**, 453 (1964). d) E. L. Fasanella and W. Gordy, *Proc. Natl. Acad. Sci. U. S. A.*, **62**, 299 (1969).

21 a) P. P. Levin, V. Ya. Shafirovich, and V. A. Kuzmin, *J. Phys. Chem.*, **96**, 10044 (1992). b) P. P. Levin, V. Ya. Shafirovich, E. E. Batova, and V. A. Kuzmin, *Chem. Phys. Lett.*, **228**, 357 (1994).

22 K. M. Salikhov, "Magnetic Isotope Effect in Radical Reactions : An Introduction," Springer-Verlag, Wien (1996).

23 Y. Tanimoto, Y. Fujiwara, S. Takamatsu, A. Kita, M. Itoh, and M. Okazaki, *J. Phys. Chem.*, **96**, 9844 (1992).

24 U. E. Steiner and J. Q. Wu, *Chem. Phys.*, **162**, 53 (1992).